PSFC/JA-10-14

Millimeter-Wave Radiometer Diagnostics of Harmonic Electron Cyclotron Emission in the Levitated Dipole Experiment (LDX)

P. P. Woskov, J. Kesner, D. T. Garnier*, and M. E. Mauel*

* Columbia University, New York, NY 10027, USA

June 2010

Plasma Science and Fusion Center
Massachusetts Institute of Technology
Cambridge MA 02139 USA

This work was supported by the U.S. Department of Energy, Grant No. DE-FG02-98ER54458. Reproduction, translation, publication, use and disposal, in whole or in part, by or for the United States government is permitted.

Millimeter-Wave Radiometer Diagnostics of Harmonic Electron Cyclotron Emission in the Levitated Dipole Experiment (LDX)

P. P. Woskov,[1] J. Kesner[1], D. T. Garnier[2], and M. E. Mauel,[2]
[1]*Plasma and Science Fusion Center, MIT, Cambridge, MA 02139, USA*
[2]*Columbia University, New York, NY 10027, USA*

A 110/137 GHz radiometer pair with collimated antenna pattern is being used to diagnose optically thin harmonic electron cyclotron emission (ECE) from hot electrons in LDX. Signal levels of 0.1-1 keV and 110/137 ratios of 2-4 stationary with ECRH power have been observed. The large plasma core magnetic field gradient causes all relevant harmonics to be simultaneously viewed over a $\angle(\mathbf{k}, \mathbf{B})$ angular range of 0-90° representing a unique geometry for interpretation of ECE in terms of hot electron temperature and density.

I. INTRODUCTION

The detection and interpretation of harmonic electron cyclotron emission (ECE) from a magnetic dipole plasma is being investigated at LDX. The plasma in LDX is confined on closed flux surfaces surrounding the outside of a 1.1 MA, R=39 cm, a=17 cm free floating superconducting coil (F-coil) inside a 5 m diameter vacuum chamber. Unlike plasmas confined inside a set of coils, plasma turbulence in a dipole plasma acts to sustain a highly peaked profile[1] that may be ideal for advance cycle fusion reactors[2].

Though the field configuration is a simple dipole, the interpretation of ECE diagnostics is much more complex than with plasmas inside a set of coils. This is because any view from the outside encompasses a broad range of magnetic field strengths and view angles $\angle(\mathbf{k}, \mathbf{B})$ encompassing many ECE harmonics. Previous measurements with 110, 137, and 165 GHz radiometers viewed the plasma vertically from the bottom near the axis through an obstructing coil catcher or near horizontally aimed at the low field midpane[3]. It was found that the lowest ECE harmonic on the density peak anywhere within the fringe of view would dominate the observed signal.

In the present work a 110/137 GHz radiometer pair has been oriented for an unobstructed view centered on the strongest ECE above the F-coil as seen from a port located at r=275 cm and z=30.5 cm just above the outside midplane as shown in Fig. 1. The heavy partial flux contour shown (C-shaped) near the inner closed flux surface going through the inside of the F-coil traces the approximate density peak in the magnetic field range of 0.3 – 3.0 Tesla corresponding to the ECE harmonic range of 2nd – 12th at 110 GHz. Higher outside harmonics are extremely weak and can be safely ignored. The highly peaked LDX plasma profile[1] localizes the detected 110/137 GHz ECE to this flux surface. The strongest field region above 2.0 Tesla is blocked from direct view by the F-coil, but may be a factor via wall reflections.

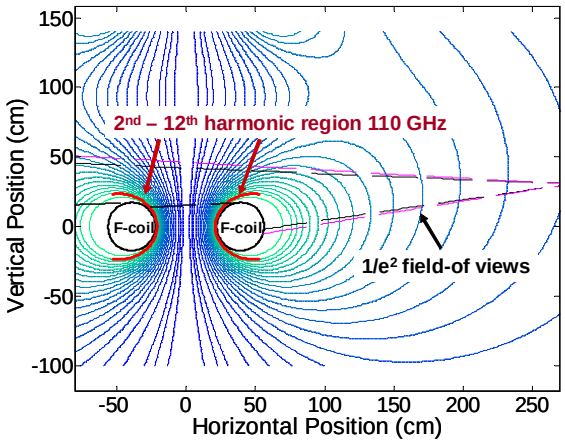

FIG. 1. Poliodal cross section of LDX F-coil, flux surface contours, 110/137 GHz radiometer field of views, and ECE source location (r, horizontal axis and z, vertical axis).

II. INSTRUMENTATION

Heterodyne receivers centered at 110 and 137 GHz, were combined into a single field of view as shown in Fig. 2 using 20 mm internal diameter corrugated aluminum waveguide and a four port corrugated waveguide beam combiner block. The beam combiner used a 1 mm thick fused quartz plate at 45° having approximately 50% transmission at both 110 and 137 GHz for polarization perpendicular to the plane of incidence (perp. to Fig. 2). The fourth port was terminated to a room temperature blackbody[4]. The maximum waveguide length with one miter bend from the 137 GHz receiver to the output aperture was about 45 cm. A 7° corrugated up taper increased the waveguide launch aperture to 28.6 mm diameter at the fused quartz vacuum window on LDX. The $1/e^2$ diameter diffracting Gaussian field of view from this launch aperture is plotted in Fig. 1 for the 110 GHz (outer) and 137 GHz (inner) frequencies.

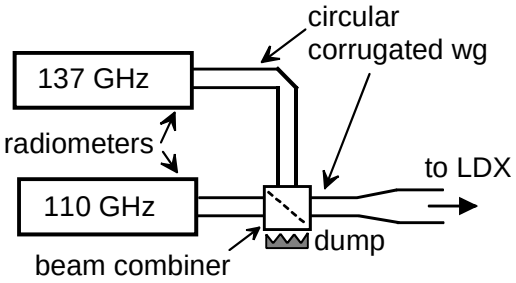

FIG. 2. 110/137 GHz receiver pair combined field of view.

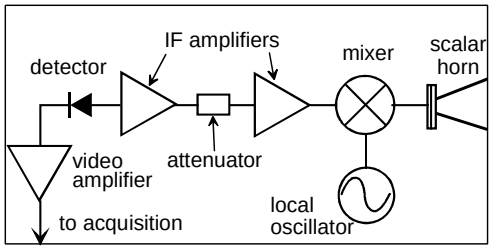

FIG. 3. General circuit for each receiver in shield enclosure

The general circuit for each receiver is shown in Fig. 3. The receiver front ends were different with the 110 GHz receiver using a fundamental 110 GHz local oscillator (LO) and the 137 GHz receiver operated subharmonically with a 68.5 GHz LO. However, identical components were used in the intermediate frequency (IF) arm of each receiver so that they would behave similarly over a wide signal dynamic range. The IF components in order from the mixer are: a 0.5 – 2.0 GHz 40 dB gain bipolar MITEQ amplifier, a changeable attenuator, a Mini Circuits ZKL-2 29 dB gain amplifier, a zero bias Schottky diode, and a 30 dB gain video amplifier used for isolation to the data acquisition system. All these receiver components were enclosed inside an aluminum box that was electrically isolated from the circuit components for noise shielding.

III. CALIBRATION

The receivers were calibrated to take into account nonlinearity to quantitively follow the ECE from small start up and afterglow levels of < 1 eV to intense ECE of > 1000 eV during full power sustained plasmas. The small signal calibration of both receivers including the beam combiner was obtained by viewing a liquid nitrogen blackbody[4] at the waveguide launch aperture with the up taper and 28.6 mm waveguide section removed.

The high power response was calibrated at the Schottky diode detector with a ~25 mW microwave Gunn oscillator source that was attenuated in steps to over 40 dB. An Agilent EPM Series Power Meter was used at each step to determine the power input to the detector. The nonlinearity of the IF amplifiers was not considered because the maximum amplified signal was estimated to be low the +15 dBm 1 dB compression point of the output IF amplifier. Fig. 4 shows the experimental points obtained for the high power calibration normalized to the small signal calibration obtained with a 6 dB attenuator between the IF amplifiers.

A second order calibration equation was needed to fit a curve to the experimental data. The resulting calibration equation is given by:

$$KT_{in} = V_{out}\left(1+\alpha V_{out}\right) \qquad (1)$$

where T_{in} is the signal input at the waveguide aperture in eV, V_{out} is the voltage output of the video amplifier in mV, K is the small signal response, and α is the second order response term. Table I lists the calibration parameters that were determined for the two receivers with a 10 dB and a 6 dB attenuator between the IF amplifiers.

The transmission through the LDX fused quartz vacuum window was also measured at the incident angles used in the

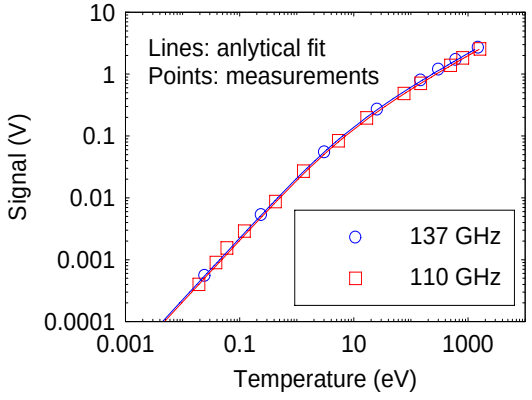

FIG. 4. Calibration of each receiver with 6 dB IF attenuator.

TABLE I. Calibration Parameters

Frequency (GHz)	K (mV/eV)	α	Window Transmission
Shots 100128001 – 100129056 (10 dB Atten., 3° Tilt)			
110 137	10.159 10.212	0.004363 0.004760	0.93 0.98
Shots 90722001 - 90722032 (6 dB Atten., 8° Tilt)			
110 137	22.547 20.764	0.004363 0.004760	0.86 0.97

experiments. This was done with a liquid nitrogen blackbody source and the window removed form the vacuum chamber. The measured signals presented here were corrected for window transmission.

IV. MEASUREMENTS

A representative example of the ECE from a D_2 plasma is shown in Fig. 5a with the viewing geometry of Fig. 1 and all LDX ECRH sources turned on for a combined power of 26.9 kW. The sequencing and individual power of the sustaining sources is shown in Fig. 5b. The 110 and 137 GHz ECE peaks at about 800 and 300 eV, respectively. The ECE and electron density both peak during the on time of the 10 kW, 10.5 GHz klystron source between 2 and 10 seconds as indicated by arrows A and B. The peak line integrated electron density was about 4.3 X 10^{13} cm^{-2} for this shot. The 10 kW, 28 GHz gyrotron which remains on through 12 seconds does not sustain the high ECE level.

Except for the gyrotron source, the ECE levels show a strong dependence on ECRH power. Without both the 10.5 and 6.4 GHz sources on they are down by about a factor of four as shown for 110 GHz signal in lower trace of Fig. 5a. The peak line integrated density is down only about 50% without the 10.5 and 6.4 GHz sources. At point C all ECRH sources are completely off and an afterglow with 2 second 1/e decay begins.

The main advantage of using a matched pair of receivers at different frequencies is that the ratio of the two signals will be a function of electron temperature only. Fig. 6 shows 137/110 GHz observed ratios with the 3° and 8° down tilt views in the present and pervious setups[3], respectively. The hot electron temperature responsible for the ECE does not change significantly with ECRH power as do the absolute ECE signals shown in Fig. 5 for the same shots. In fact with higher ECRH power there is some decrease in hot electron temperature which can be attributed to increasing electron density. Another characteristic feature is that the hot electron temperature rises in the afterglow as the colder electrons are preferentially lost as would be expected for collisional relaxation with the background gas.

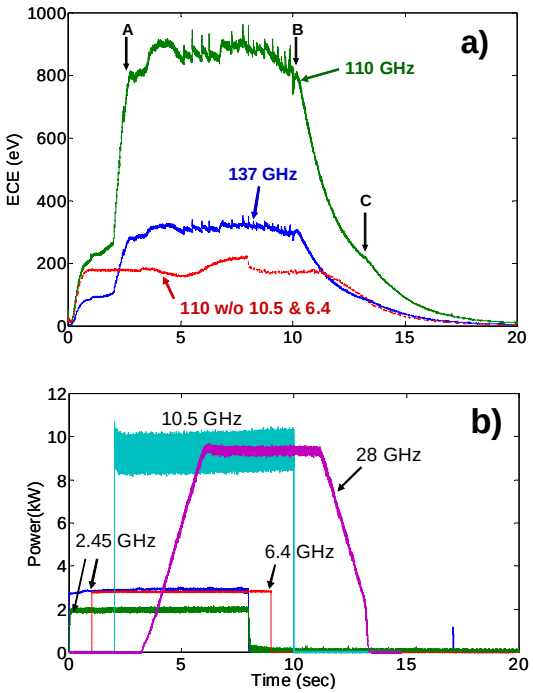

FIG. 5. a) Observed ECE for LDX plasma shots #100128017 & 22, b) ECRH power for same shots except as noted.

When the receiver field of view was tilted 8° downward the observed 137/110 GHz ratio was noticeably lower for plasmas with similar density and diamagnetism. There was no gyrotron previously, but the three traces above show that the frequency and power of ECRH is not a significant factor in determining the hot electron temperature.

V. DISSCUSION

It is well known that the electron distribution function (EDF) in ECRH sustained plasmas is non Maxwellian and various EDFs have been proposed including multi Maxwellian, loss cone, and the ECRH distribution[5]. Knowledge of the true EDF can be conveniently skirted by considering an equivalent Maxwellian EDF temperature that fits the data, which in this case limits the determination to the high energy tail temperature of the electrons. Such an analysis was carried out for the 8° downward viewed ECE assuming wall reflections could be ignored[3]. Applying the same analysis to the present 3° downward data has shown that wall reflection can not be ignored. If the millimeter-wave ECE hot electron temperature is an approximate invariant with ECRH power and frequency as the data in Fig. 6 suggests, then the 3° ratio data should have fallen in the 0.7 – 0.6 range, but instead it is

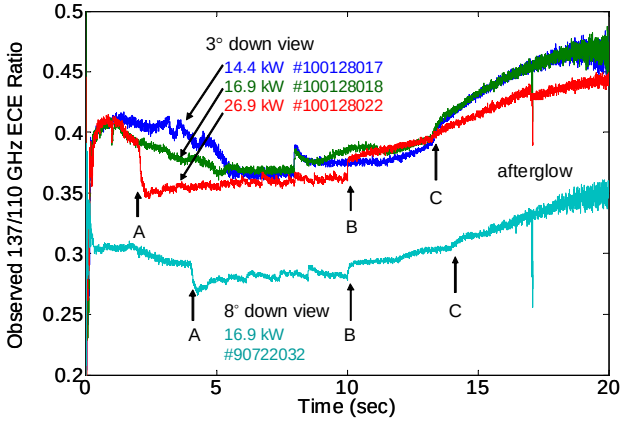

FIG. 6. Observed 137/110 GHz ECE ratio at different ECRH power levels and view directions.

only about half that. Furthermore the absolute ECE levels should have been much larger for the direct view of the high field region, but instead they are about the same[3].

It is likely that the previous data looking into the low field region would have been affected more by reflections than the present measurements looking directly into the strong ECE region. If that is the case then the millimeter-wave hot electron temperatures would be lower than previously estimated by a factor of 2 or more to < 40 keV during sustained ECRH.

In order to convert the observed 110/137 GHz ratio data into a more accurate hot electron temperature it will be necessary to consider the ECE from the inside of the F-coil not in direct view and to determine a refection factor to add this component to the ratio-temperature conversion curve. This will be a subject of future analysis. Once a determination of the actual hot electron temperature is made, then it can be used with the observed absolute ECE levels to back out a hot electron density. Wall reflections again will need to be considered because the ECE source region in direct view does not fill the receiver views as an examination of Fig. 1 shows. A reflection fill factor will need to be determined to correct the actual emission levels at the plasma.

In summary, we have observed the following: 1) LDX emits a high level of harmonic ECE revealing a significant population of hot electrons, 2) the hot electron temperature is not a significant function of ECRH power or frequency, 3) the hot electron density is a significant function of ECRH power and frequency, and 4) the sustained hot electron temperature may be lower than previously estimated due to wall reflections contributing to the observed ECE.

REFERENCES AND FOOTNOTES

[1] A. C. Boxer, R. Bergmann, J. L. Ellsworth, D. T. Garnier, J. Kesner, M. E. Mauel and P. Woskov, Nature Physics **6**, 207 (2010).

[2] J. Kesner, D. T. Garnier, A. Hansen, M. E. Mauel and L. Bromberg, Nuclear Fusion **44** 193 (2004).

[3] P. P. Woskov, J. Kesner, D. T. Garnier, M. E. Mauel and S. H. Nogami, LAPD14, Journal of Physics: Conference Series, to be published (2010).

[4] carbon impregnated pyramidal foam such as ECCOSORB, Emerson & Cuming.

[5] R. C. Garner, M. E. Mauel, S. A. Hokin, R. S. Post and D. L. Smatlak, Phys. Rev. Lett. **59** 1821 (1987).